



ELSEVIER

Engineering Analysis with Boundary Elements 28 (2004) 825–832

ENGINEERING
ANALYSIS *with*
BOUNDARY
ELEMENTS

www.elsevier.com/locate/enganabound

Complex variable BEM for thermo- and poroelasticity

Vadim Koshelev^a, Ahmad Ghassemi^{b,*}

^a*Institute for Problems of Mechanical Engineering, Russian Academy of Sciences, St-Petersburg 199178, Russia*

^b*University of North Dakota, Room 330A, Leonard Hall, Grand Forks 58202, USA*

Received 5 June 2003; revised 11 July 2003; accepted 26 August 2003

Abstract

A stationary thermoelastic (poroelastic) boundary element method is suggested based on the Complex Variable Hypersingular Boundary Integral Equation. The method is developed for heterogeneous blocky media. Various conditions on the contacts between the blocks are considered, namely discontinuity of temperature (pore pressure) or discontinuity of heat (fluid) flux. The problem of the basic integrals calculation is discussed and numerical examples are presented to demonstrate the potential of the method.

© 2003 Elsevier Ltd. All rights reserved.

Keywords: Thermoelasticity; Poroelasticity; Boundary element method; Complex variables

1. Introduction

Many problems of mechanics of materials, in general and geomechanics in particular, deal with the stress and displacement calculations for heterogeneous media consisting of blocks, grains and inclusions. These problems often involve thermal and pore pressure effects. Heterogeneity of both mechanical and thermal (or poromechanical) characteristics necessitates numerical analysis of the problem of interest. The Boundary Element Method (BEM) based on the Hypersingular Boundary Integral Equations (BIE) has shown to be the most effective technique for treatment of problems with complicated contact conditions. In this work, the Complex Variable (CV) Hypersingular BIE [1,2] is utilized. The equation is formulated in the terms of direct values of integrals. An alternative treatment without involving the direct value of a finite part integral can be found in other works [3,4] that use the Hadamard type integral which is a derivative of Cauchy type integral.

The equation under consideration contains displacements discontinuities and tractions on the boundaries of the blocks. Thus, there is no need to use additional relations to calculate the characteristics of the contacts interaction as in the case of Singular Equations. The CV-BEM presented herein has been developed by considering additional terms that depend on the given values of a potential (temperature or pore

pressure) and its normal derivative (heat or fluid flux) at the boundary of the domain under consideration. These values may be found using the CV-BEM for potential problems [5].

2. Integral identities of direct BEM

Below, we deal with BIE and the direct formulation BEM. Their derivation is based on the reciprocity theorem of work. The formulation of the thermoelastic version follows [6]

$$\int_S (\sigma_i u_i^* - \sigma_i^* u_i) ds + \int_V (\psi_i u_i^* - \psi_i^* u_i) dV + \int_V \gamma (T \varepsilon_{kk}^* - T^* \varepsilon_{kk}) dV = 0, \quad (1)$$

where a repeated index implies a sum; and $(\psi_i, \sigma_i, u_i, T)$ and $(\psi_i^*, \sigma_i^*, u_i^*, T^*)$ characterize two independent states of body force, traction, displacement and temperature for the thermoelastic body V having a surface S . The coefficient γ is a constant from the constitutive equation

$$\sigma_{ij} = C_{ijkl} \varepsilon_{kl} - \gamma \delta_{ij} T. \quad (2)$$

For the poroelastic case γ is defined as Biot's effective stress coefficient [7,8]. The common method to arrive at the integral identities of the direct method is to take the actual state under consideration as the first state mentioned above; and consider the second state to be generated by a unit body

* Corresponding author. Tel.: +1701-777-3213; fax: +1701-777-4449.
E-mail address: ahmad_ghassemi@mail.und.nodak.edu (A. Ghassemi).

force applied at the point $x \in V$ and directed along the j th coordinate axis; with $T^* = 0$ in the entire body. In the last case, the displacement u_k at the point $y \in V$ is represented, the fundamental solution of the elasticity problem or Green's function $G_{kj}(x, y)$, which for an infinite plane has the form of Kelvin's solution

$$G_{kj}(x, y) = -\frac{1}{2\pi\mu(\kappa+1)} \left(\kappa\delta_{kj} \ln r - \frac{\partial r}{\partial x_k} \frac{\partial r}{\partial x_j} \right), \quad (3)$$

where $\kappa = 3 - 4\nu$ for plane strain; and $\kappa = (3 - \nu)/(1 + \nu)$ for plane stress; ν is Poisson's ratio, μ is shear modulus, and $r = |x - y|$ is the distance between x and y ; $j, k = 1, 2$; $x = (x_1, x_2)$; $y = (y_1, y_2)$. The formulae for tractions at the point $\xi \in S$ have been derived from the well-known relations between tractions and elastic displacements. It has a form

$$F_{kj}(x, \xi) = -\frac{1}{\pi(\kappa+1)} \left[\frac{\kappa-1}{2} \left(n_j \frac{\partial r}{\partial x_k} - n_k \frac{\partial r}{\partial x_j} \right) + \left(\frac{\kappa-1}{2} \delta_{kj} + 2 \frac{\partial r}{\partial x_k} \frac{\partial r}{\partial x_j} \right) \frac{\partial r}{\partial x_l} n_l \right], \quad (4)$$

where n_j is the normal vector at the point ξ .

Thereby, after the conventional transformations of the first two integrals in Eq. (1) we arrive at the well-known identity that includes an additional integral term with potential function p (temperature or pressure) on the left side

$$\int_S [\sigma_k(x)G_{kj}(x, \xi) - F_{kj}(x, \xi)u_k(x)]dS_x + \int_V \psi_k(y)G_{kj}(y, \xi)dV_y + \int_V \gamma p(y) \frac{\partial G_{kj}(y, \xi)}{\partial y_k} dV_y = u_j(\xi). \quad (5)$$

The mentioned volume integral is converted [9] to a surface integral because the temperature (pore pressure) is a harmonic function. The final integral identities of the direct BEM are

$$\int_S [\sigma_k(x)G_{kj}(x, \xi) - F_{kj}(x, \xi)u_k(x)]dS_x = u_j(\xi) + \int_S \left[G_j(x, \xi) \gamma \frac{\partial p(x)}{\partial n} - F_j(x, \xi) \gamma p(x) \right] dS_x \quad (6)$$

where the kernels of the integral on the R.H.S. are

$$G_j(x, \xi) = \frac{\partial \Phi}{\partial x_j}; \quad F_j(x, \xi) = \frac{\partial G_j}{\partial n}, \quad (7)$$

with

$$\Phi = \frac{\kappa-1}{8\pi\mu(\kappa+1)} r^2 (1 - \ln r).$$

Here and below we do not consider for simplicity the body forces ψ_k . Thereby, Eq. (6) does not contain the second integral from Eq. (5).

3. Complex Variables BIE

We choose one of the techniques available for formulating the CV-BIE [1–2]. Namely, we multiply the expression (6) for the case of $j = 2$, by the imaginary unit and add it to the corresponding expression for $j = 1$. Then, we rearranged terms on the R.H.S. of the resulting equation to obtain the conventional kernels in CV-BIE. Thus, we have

$$\frac{1}{2\pi i} \int_S \left\{ (\kappa-1) \frac{u(\tau)}{\tau-z} d\tau + u(\tau) dk_1(\tau, z) + \bar{u}(\tau) dk_2(\tau, z) - 2\kappa \frac{\sigma(\tau)}{2\mu} \ln(\tau-z) d\tau + \kappa \frac{\sigma(\tau)}{2\mu} k_1(\tau, z) d\tau - \frac{\bar{\sigma}(\tau)}{2\mu} k_2(\tau, z) d\bar{\tau} \right\} = (\kappa+1)u(z) + P_C(z), \quad (8)$$

where $P_C(z)$ is the transformed body potential

$$P_C(z) = (\kappa+1) \int_S \left[G_C(\tau, z) \gamma \frac{\partial p(\tau)}{\partial n} - F_C(\tau, z) \gamma p(\tau) \right] ds, \quad (9)$$

$$G_C(\tau, z) = G_1(x, \xi) + iG_2(x, \xi) = \frac{\kappa-1}{8\pi\mu(\kappa+1)} (\tau-z)(1 - \ln r^2), \quad (10)$$

$$F_C(\tau, z) ds = [F_1(x, \xi) + iF_2(x, \xi)] ds = \frac{i(\kappa-1)}{8\pi\mu(\kappa+1)} (\ln r^2 d\tau - k_2 d\bar{\tau}), \quad (11)$$

τ and $z(\tau \in S, z \in V)$ are complex coordinates of points x and ξ ; $\tau = x_1 + ix_2$; $z = \xi_1 + i\xi_2$; $\sigma(t) = \sigma_{nn} + i\sigma_{nt}$ is a complex traction in a local coordinates system at the boundary (normal and shear components); $u(\tau) = u_1 + iu_2$. The kernels of the integrals in Eq. (8) are

$$k_1(\tau, z) = \ln \frac{\tau-z}{\bar{\tau}-\bar{z}}; \quad k_2(\tau, z) = \frac{\tau-z}{\bar{\tau}-\bar{z}}. \quad (12)$$

The bar over a symbol denotes complex conjugation.

The identity (8) yields the Singular CV-BIE when one takes a limit as $z \rightarrow t$, where $t \in S$. According to the theory of Singular integrals, this operation generates an additional term $(\kappa+1)u(t)/2$ on the left hand side of the equation. As a result we have

$$\frac{1}{2\pi i} \int_S \left\{ (\kappa-1) \frac{u(\tau)}{\tau-t} d\tau + u(\tau) dk_1(\tau, t) + \bar{u}(\tau) dk_2(\tau, t) - 2\kappa \frac{\sigma(\tau)}{2\mu} \ln(\tau-t) d\tau + \kappa \frac{\sigma(\tau)}{2\mu} k_1(\tau, t) d\tau - \frac{\bar{\sigma}(\tau)}{2\mu} k_2(\tau, t) d\bar{\tau} \right\} = \frac{1}{2}(\kappa+1)u(t) + P_C(t). \quad (13)$$

As it was pointed out earlier, the hypersingular equation is more proper for our aims; it may be obtained by applying the operator T_z of complex tractions to both parts of Eq. (8) and subsequently taking the limit as $z \rightarrow t$. T_z corresponds to the site with a tangent vector $\exp(iaz)$ and acts

as follows [10]

$$T_z U(z, \bar{z}) = 2\mu \left[\frac{1}{\kappa - 1} \left(\frac{\partial U}{\partial z} + \frac{\partial \bar{U}}{\partial \bar{z}} \right) - \exp(-2i\alpha_z) \frac{\partial U}{\partial \bar{z}} \right]. \quad (14)$$

The result of its action on both parts of Eq. (8) is a hypersingular entity

$$2\mu \mathbf{H}_z(u, \sigma) = (\kappa + 1)\sigma(z) + (\kappa + 1)\gamma p(z) + T_z P_C(z), \quad (15)$$

where

$$\begin{aligned} \mathbf{H}_z(u, \sigma) = & \frac{1}{2\pi i} \int_S \left\{ \frac{2u(\tau)}{(\tau - z)^2} d\tau - u \frac{\partial}{\partial z} dk_1(\tau, z) \right. \\ & - \bar{u}(\tau) \frac{\partial}{\partial z} dk_2(\tau, z) - \frac{\kappa - 1}{2\mu} \frac{\sigma(\tau)}{\tau - z} d\tau - \kappa \frac{\sigma(\tau)}{2\mu} \frac{\partial k_1}{\partial z} d\tau \\ & \left. + \frac{\bar{\sigma}(\tau)}{2\mu} \frac{\partial k_2}{\partial z} d\bar{\tau} \right\}, \quad (16) \end{aligned}$$

$$\frac{\kappa + 1}{2\mu} T_z P_C(z) = \frac{\kappa + 1}{2\mu} \int_S \left[T_z G_C(\tau, z) \frac{\partial p(\tau)}{\partial n} - T_z F_C(\tau, z) p(\tau) \right] ds, \quad (17)$$

$$\frac{\kappa + 1}{2\mu} T_z G_C(z) = \frac{1}{8\pi\mu} [2\ln r^2 - \exp(-2i\alpha_z)(\kappa - 1)k_2(\tau, z)], \quad (18)$$

$$\begin{aligned} \frac{\kappa + 1}{2\mu} T_z F_C(z) ds = & \frac{i(\kappa - 1)}{8\pi\mu} \left[\frac{2d\tau}{\tau - z} + \frac{\partial k_1}{\partial z} d\tau + \frac{\partial k_2}{\partial z} d\bar{\tau} \right. \\ & \left. + \frac{\kappa + 1}{\kappa - 1} \left(\frac{d\bar{\tau}}{\bar{\tau} - \bar{z}} - \frac{d\tau}{\tau - z} \right) \right]. \quad (19) \end{aligned}$$

Thereafter, we take the limit as $z \rightarrow t$ of both parts of Eq. (15). Integrals on the left hand side transform into finite part integrals [2,3] and principal value integrals. An additional term $(\kappa + 1)\sigma(t)/2$ appears due to singularity. Also, $P_C(z)$ contains a singular kernel in $T_z F_C(\tau, z)$. Thus, one has to follow the general rule of taking a limit: $T_t P_C = \lim T_z P_C$ as $z \rightarrow t$. Besides, we take into account that in the right hand side $T_z u(z) = \sigma(z) + \gamma p(z)$; according to the constitutive Eq. (2) of thermo- (or poro) elasticity.

Finally, we obtain the hypersingular integral equation

$$\mathbf{H}_t(u, \sigma) = \frac{1}{2} \frac{\kappa + 1}{2\mu} \sigma(t) + \frac{1}{2} \frac{\kappa + 1}{2\mu} \gamma p(t) + \frac{\kappa + 1}{2\mu} T_t P_C, \quad (20)$$

where

$$\begin{aligned} \mathbf{H}_t(u, \sigma) = & \frac{1}{2\pi i} \int_S \left\{ \frac{2u(\tau)}{(\tau - t)^2} d\tau - u(\tau) \frac{\partial}{\partial t} dk_1(\tau, t) \right. \\ & - \bar{u}(\tau) \frac{\partial}{\partial t} dk_2(\tau, t) - \frac{\kappa - 1}{2\mu} \frac{\sigma(\tau)}{\tau - t} d\tau \\ & \left. - \kappa \frac{\sigma(\tau)}{2\mu} \frac{\partial k_1}{\partial t} d\tau + \frac{\bar{\sigma}(\tau)}{2\mu} \frac{\partial k_2}{\partial t} d\bar{\tau} \right\}, \quad (21) \end{aligned}$$

$$\frac{\kappa + 1}{2\mu} T_t P_C \equiv \mathbf{K}_t p + \mathbf{L}_t \frac{\partial p}{\partial n} = \int_S \gamma p(\tau) dK(\tau, t) + \int_S \gamma \frac{\partial p}{\partial n}(\tau) dL(\tau, t), \quad (22)$$

$$\begin{aligned} dK(\tau, t) = & \frac{i(\kappa - 1)}{8\pi\mu} \left[\frac{2d\tau}{\tau - t} + \frac{\partial k_1}{\partial t} d\tau + \frac{\partial k_2}{\partial t} k_2(\tau, t) d\bar{\tau} \right. \\ & \left. + \frac{\kappa + 1}{\kappa - 1} \left(\frac{d\bar{\tau}}{\bar{\tau} - \bar{t}} - \frac{d\tau}{\tau - t} \right) \right], \quad (23) \end{aligned}$$

$$dL(\tau, t) = \frac{1}{8\pi\mu} [2\ln r^2 - \exp(-2i\alpha_t)(\kappa - 1)k_2(\tau, t)], \quad (24)$$

where $r^2 = |\tau - t|^2$. Eq. (20) modifies the well-known CVH-BIE [1,2] for thermoelasticity and poroelasticity. It includes two new terms on the R.H.S. that take into account a given distribution of potential function (temperature or pore pressure) and its normal derivation (flux) distributed over the domain's boundary.

4. BIE for blocky media

Consider a medium consisting of a number of blocks with different mechanical and thermal characteristics. These blocks may be surrounded by an external domain (matrix), which extends to infinity (Fig. 1).

The conventional method of constructing the BIE [2] for blocky systems is to write down an equation similar to Eq. (13) or Eq. (20) for each block and the matrix. In brief, the resulting equation is as follows

$$\mathbf{H}_t^j(u, \sigma) = \frac{1}{2} \frac{\kappa + 1}{2\mu} \sigma(t) + \frac{1}{2} \frac{\kappa + 1}{2\mu} \gamma p(t) + \mathbf{K}_t^j p + \mathbf{L}_t^j \frac{\partial p}{\partial n}, \quad (25)$$

where \mathbf{K}_t^j and \mathbf{L}_t^j are the integral operators acting on the potential and the flux, respectively; j is a number of the block with a boundary S_j . Then, the equations for the blocks are summed to arrive at the integral equation, where S is the total boundary consisting of the boundaries between all pairs of neighboring blocks. Every part of S is traversed twice, in opposite directions. Thus, we consider one direction as positive (+) and the other as negative (-).

$$\begin{aligned} \frac{1}{2\pi i} \int_S \left\{ \frac{2\Delta u}{(\tau - t)^2} d\tau - \Delta u \frac{\partial}{\partial t} dk_1 - \Delta \bar{u} \frac{\partial}{\partial t} dk_2 \right. \\ \left. + (2a_1 - a_3) \frac{\sigma d\tau}{\tau - t} + (a_1 - a_3) \sigma \frac{\partial k_1}{\partial t} d\tau + a_1 \bar{\sigma} \frac{\partial k_2}{\partial t} d\bar{\tau} \right\} \\ = \frac{a_2}{2} \sigma(t) + s^\infty + \frac{1}{2} \frac{\kappa^+ + 1}{2\mu^+} p^+(t) - \frac{1}{2} \frac{\kappa^- + 1}{2\mu^-} p^-(t) \\ + \mathbf{K}^+ p^+ - \mathbf{K}^- p^- + \mathbf{L}^+ \frac{\partial p^+}{\partial n} - \mathbf{L}^- \frac{\partial p^-}{\partial n}, \quad (26) \end{aligned}$$

where

$$\begin{aligned} a_1 = & \frac{1}{2\mu^+} - \frac{1}{2\mu^-}; \quad a_2 = \frac{\kappa^+ + 1}{2\mu^+} + \frac{\kappa^- + 1}{2\mu^-}; \\ a_3 = & \frac{\kappa^+ + 1}{2\mu^+} - \frac{\kappa^- + 1}{2\mu^-}, \end{aligned}$$

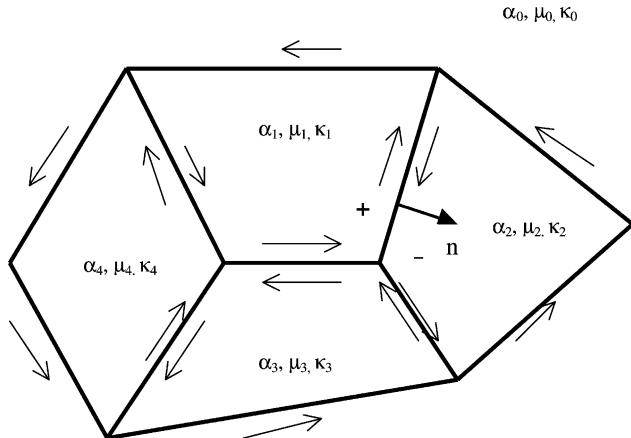


Fig. 1. A sketch of a blocky system with direction of traversal for the boundaries of each block.

and

$$s^\infty = -\frac{\kappa_0 + 1}{2\mu_0} [\sigma_1^\infty + \sigma_2^\infty + \exp(-2i\alpha_l)(\sigma_2^\infty - \sigma_1^\infty - 2i\sigma_{12}^\infty)].$$

In Eq. (26), we have omitted the summation symbol over different parts of the total contour S . But, it is implicitly included because the mechanical parameters under the integral are considered as variables. The sign over the operators indicates that they depend on the parameters to the left (+) or to the right (-) from the direction of traverse: $\mathbf{K}^\pm, \mathbf{L}^\pm \rightarrow \alpha^\pm, \mu^\pm, \kappa^\pm$.

The left side of Eq. (26) corresponds to the case of continuous tractions on the boundaries of the blocks. On the contrary, the presence of the $\Delta u = u^+ - u^-$ means that displacement discontinuity may occur at some parts of the contour. The R.H.S. of Eq. (26) presents a general case of continuity or discontinuity of the fields under consideration. A number of various situations are possible at every part of S : continuity or discontinuity of the mechanical and thermal characteristics and/or continuity or discontinuity of the potential and flux.

Let us consider some particular cases of formulae (25). If $p^+ = p^- = p$, then $\mathbf{K}^+ p^+ - \mathbf{K}^- p^- = (\mathbf{K}^+ - \mathbf{K}^-)p$. This term vanishes also if $\mathbf{K}^+ = \mathbf{K}^-$ in the case of blocks with the identical properties: $\alpha^+ = \alpha^-$; $\kappa^+ = \kappa^-$; $\mu^+ = \mu^-$. Suppose we have $\mathbf{K}^+ = \mathbf{K}^- = \mathbf{K}$ but $p^+ - p^- = \Delta p \neq 0$; then, Eq. (25) reduces to: $\mathbf{K}^+ p^+ - \mathbf{K}^- p^- = \mathbf{K} \Delta p$. This is the case of a thermal inclusion in thermoelasticity or a discontinuity of pore pressure in poroelasticity. A similar cases may be considered for \mathbf{L}^\pm and $\partial p^\pm / \partial n$.

5. Examples

1. The numerical procedures described above are applied to a number of examples. First, consider a mechanically homogeneous infinite plane with a circular inclusion (Fig. 2). On the boundary of the inclusion,

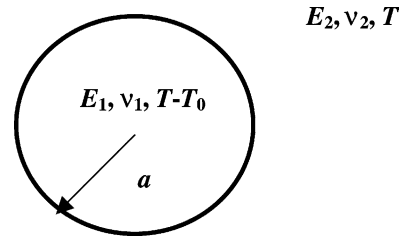


Fig. 2. A circular inclusion in an infinite plane.

the temperature field experiences a discontinuity: $T(r) = T_0$ if $r < a$; and $T(r) = 0$ if $r \geq a$. The analytical results for this case of an axisymmetric thermal inclusion is given in Nowacki [6]

$$\sigma_{rr} = \sigma_{\varphi\varphi} = -\mu m T_0, \quad \text{if } r < a, \quad (27)$$

$$\sigma_{rr} = -\sigma_{\varphi\varphi} = -\mu m T_0 \frac{a^2}{r^2}, \quad \text{if } r \geq a,$$

$$m = \alpha \frac{7 - \kappa}{\kappa + 1}.$$

In the numerical test for plane strain, we assume that: $\nu = 0.25$; $E = 1$; $\kappa = 3 - 4\nu = 2$; $m = 5\alpha/3 = 1.6667\alpha$; $T_0 = 100$; $\alpha = 0.01$; $\mu = 0.5E/(1 + \nu) = 0.5 \times 4 \times E/(7 - \kappa)$. So, $\mu m T_0 = 2E\alpha T_0/(\kappa + 1) = 2/3 = 0.66667$. Finally, the stresses inside the inclusion are $\sigma_{rr} = \sigma_{\varphi\varphi} = -0.66667$, whereas for the region outside the circle we have: $\sigma_{rr} = -\sigma_{\varphi\varphi} = -0.66667/r^2$.

The results of our computations for five internal points when $0.01 < r/a < 1$ coincide with the above analytical results. The values in Table 1 demonstrate good agreement between analytical and numerical data for different values of r/a . It is worth noting that good accuracy of numerical results was achieved by using only 20 segments in boundary discretization (60 collocation points). To consider the points in closed vicinity of the boundary ($r/a < 1.02$) a finer mesh of segments should be exploited.

2. Consider the case of a long thick-walled porous cylinder. Its cross-section is a circular ring $R_2 \leq r \leq R_1$. The water pressure inside the boundary of the borehole, $r = R_2$ is kept constant at $p = p_0$ and it is set to $p = 0$ at the outside of the ring (Fig. 3).

One can find the solution of the similar thermoelastic problem in Ref. [6] expressing the radial dependence of displacement on r according to

$$v(r) = m \left[\frac{1}{r} \int_{R_2}^r T(x)x dx + \frac{1}{R_1^2 - R_2^2} \left(\frac{R_2^2}{r} + \frac{\mu r}{\lambda + \mu} \right) J \right], \quad (28)$$

where

$$T = T(r) = T_0 \frac{\ln R_1 - \ln r}{\ln R_2 - \ln R_1}; \quad J = \int_{R_2}^{R_1} T(x)x dx; \quad \lambda = \frac{2\mu\nu}{1 - 2\nu}.$$

Table 1
Comparison of analytical (27) and numerical (CV-BEM) results for a thermal inclusion

	r/a	1.03	1.05	1.10	1.25	1.50	2.50	5.00
$-\sigma_{rr}; \sigma_{\varphi\varphi}$	Analytical	0.62840	0.60469	0.55096	0.42667	0.29630	0.10667	0.02667
$-\sigma_{rr}; \sigma_{\varphi\varphi}$	CV-BEM	0.62821	0.60450	0.55079	0.42654	0.29621	0.10663	0.02666

To obtain the poroelastic solution, it is sufficient to substitute the pressure, p , and $\gamma(1 + \nu)/E$ for temperature and m , respectively, in Eq. (28). Thereby, the following expressions are obtained for $\nu(R_1)$ and $\nu(R_2)$

$$\begin{aligned} \nu(R_1) &= \gamma \frac{1 + \nu}{E} \left[\frac{1}{R_1} + \frac{R_1}{R_1^2 - R_2^2} \left(\frac{R_2^2}{R_1^2} + \frac{\mu}{\lambda + \mu} \right) \right] J; \\ \nu(R_2) &= \gamma \frac{1 + \nu}{E} \frac{R_2}{R_1^2 - R_2^2} \left(1 + \frac{\mu}{\lambda + \mu} \right) J. \end{aligned} \quad (29)$$

To test the BEM calculation, consider $R_1/R_2 = 2$ and assume that other parameters are the same as in the previous example. The result is as follows: $\nu(R_1)/R_1 = \nu(R_2)/R_2 = 0.48502(1 - \nu)\gamma p_0/E$. If $\gamma = p_0 = 1$, then $\nu(R_1)/R_1 = \nu(R_2)/R_2 = 0.36377$. As before, both the internal and external circles were divided into 20 elements. For the above mentioned data, the numerically determined displacements are: $\nu(R_1)/R_1 = \nu(R_2)/R_2 = 0.36378$. Thus, the thermoelastic BEM provides the same accuracy as the complex hypersingular BEM in elasticity.

3. Consider the case of a thermal inclusion, whose mechanical properties ($\kappa^+; \mu^+$) differ from the parameters ($\kappa^-; \mu^-$) of the matrix. All the other features of the problem are the same as in the Example 1. This axisymmetric problem has an analytical solution for the normal traction σ_n on the boundary of inclusion

$$\sigma_n = - \frac{\gamma^+ T_0}{1 + \frac{2}{\kappa^+ - 1} \frac{\mu^+}{\mu^-}}. \quad (30)$$

Table 2 contains the normalized tractions ($-\sigma_n/\gamma^+ T_0$) calculated analytically using the last formulae vs.

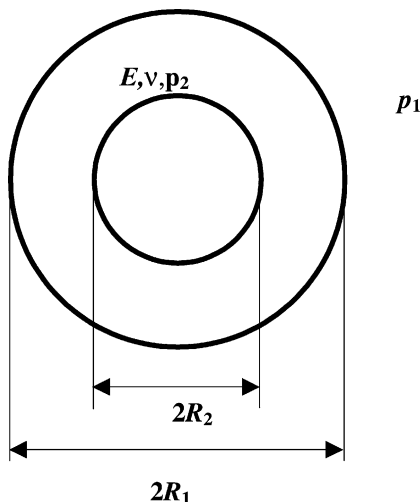


Fig. 3. Example 2, the problem of a poroelastic circular cylinder.

the results of numerical studies (CV-BEM). They correspond to the various combinations of the relation of the shear module (μ^+/μ^-) and two values of Poisson's ratio. The scheme of discretization for CV-BEM calculations was the same as in the Example 1.

This example also demonstrates good accuracy of thermoelastic BEM for inhomogeneous bodies. The level of accuracy corresponds to the results obtained earlier by CVH-BEM for mechanical inclusions.

4. The last example deals with the influence of a temperature perturbation on the stress intensity factors (SIFs) at the tips of an internal crack (Fig. 4). The crack location and the elastic properties of the inclusion (μ_2, ν_2) and the matrix (μ_1, ν_1) are the same as those in Refs. [11 and 12] (the late revision of the first one): $x(A) = -a; x(B) = -2a; y(A) = y(B) = a/2; \mu_2/\mu_1 = 23; \nu_2 = 0.30; \nu_1 = 0.35$. Firstly, we compare the SIFs for the elastic problem of a plane under uniaxial stress p applied at infinity. Our results coincide with those of Ref. [12]: $k_{I(A)} = 0.613; k_{II(A)} = 0.061; k_{I(B)} = 0.817; k_{II(B)} = -0.067$ (SIFs are normalized by $p\sqrt{\pi a/2}$).

As in the previous example, we consider a thermal inclusion whose temperature differs from the matrix temperature by ΔT (held constant). Fig. 5 presents the dependence of SIF's on the dimensionless parameter $\omega = E_2 \alpha_2 \Delta T/p$. We see that, as expected, all dependencies are linear. Heating leads to the growth of k_I at both tips and to the contrasting effect for k_{II} .

6. Conclusions

A modification of the CV Hypersingular BIE is presented for treatment of problems of thermoelasticity and poroelasticity taking into account both mechanical and thermal (poroelastic) inhomogeneity as well as possible discontinuities on the surfaces of blocks in contact. The methods for calculating the new integrals appearing on the right hand side of the BEM equations are also described. Examples are presented that demonstrate the high level of accuracy of the method illustrating the potential of thermo-(poro) elastic CVH-BEM.

Table 2
Normalized tractions on the surface of a thermo-mechanical inclusion

	$\mu^+/\mu^- =$	0.1	0.333(3)	3.0	10.0
$\kappa^+ = \kappa^- = 3$	Analytical	0.909(09)	0.75000	0.25000	0.09(09)
$(\nu^+ = \nu^- = 0.0)$	CV-BEM	0.90909	0.75000	0.25000	0.09091
$\kappa^+ = \kappa^- = 2$	Analytical	0.833(3)	0.60000	0.14286	0.04762
$(\nu^+ = \nu^- = 0.25)$	CV-BEM	0.83333	0.60000	0.14286	0.04762

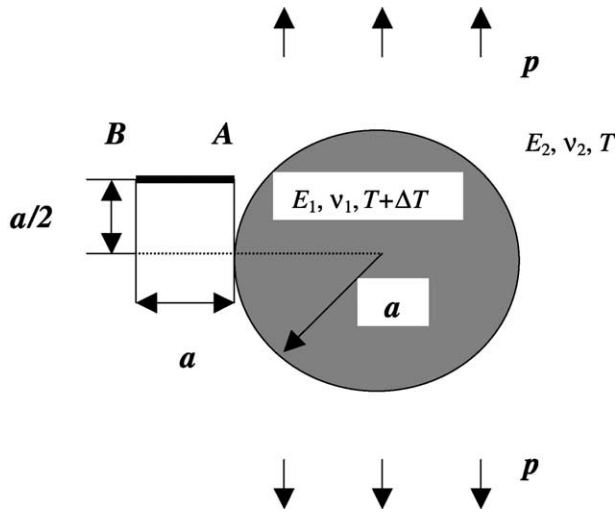


Fig. 4. The problem geometry for a thermal inclusion and a crack.

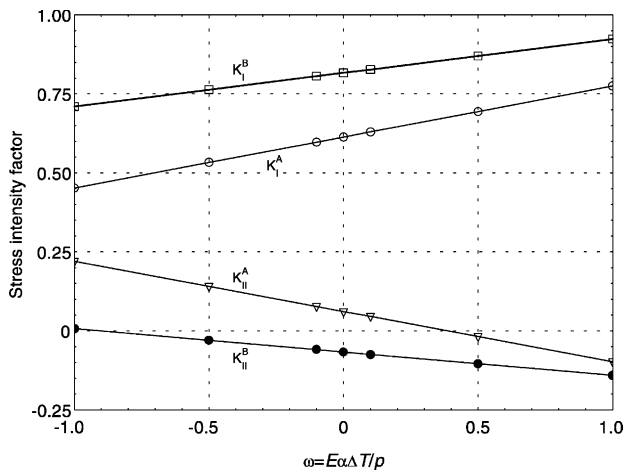


Fig. 5. Variation of stress intensity factor with parameter ω .

Acknowledgements

The financial support of the US Department of Energy under the Grant DE-FG07-99ID13855 and the ND EPSCoR through NSF grant #EPS-9874802 is gratefully acknowledged. The authors are grateful to Professor A.M. Linkov for valuable discussions. VK also expresses gratitude to the Department of Geology & Geological Engineering, University of ND for facilitating his visit to UND to work on this project.

Appendix A

New integrals calculation

The main advantage of CV-BEM as compared with the real variable methods is the simplicity of calculating the singular and hypersingular integrals over any curvilinear boundary element [1,2] for both ordinary and tip elements.

As with regular integrals, generally one can exploit numerical methods. However, for important particular cases of straight line elements and circular arc elements, regular integrals may be reduced to combinations of singular and hypersingular integrals and the derivatives of the latter [1,2].

Introducing the additional integral terms on the right part of Eq. (20), we follow the analytical approach mentioned above. The first integral with the kernel defined as dK (23) has a form

$$J_{1K} \equiv \int_Q p(\tau) dk_1(\tau, t) = \int_Q p(\tau) \frac{d\tau}{\tau - t} - \int_Q p(\tau) \frac{d\bar{\tau}}{\bar{\tau} - \bar{t}} = S_p(t) - S_p(\bar{t}), \tag{A1}$$

where $S_p(t)$ is a basic singular integral over boundary element Q . If Q is a straight element with the complex coordinate of its center, z_c , length of $2l$, and direction vector $\exp(i\alpha_c)$, then [1,2]

$$J_{1K} = S_p(t') - S_p(\bar{t}'), \tag{A2}$$

where the singular integral on the density $p(\tau)$ is as follows

$$S_p(t') = \int_{-1}^1 \frac{p(\tau') d\tau'}{\tau' - t'}; \quad t' = \exp(-i\alpha_c)(t - z_c);$$

$$\tau' = \exp(-i\alpha_c)(\tau - z_c).$$

For a circular arc with an angle $2\theta_0$ and the center coordinate, z_0 [1,2]

$$J_{1K} = S_p(0') + S_p(t') - S_p(1/\bar{t}'), \tag{A3}$$

where $t' = i \exp(-i\alpha_c)(t - z_0)/R$; $\tau' = i \exp(-i\alpha_c)(\tau - z_0)/R$; the integrals are taken in the local coordinates over the arc $2\theta_0$ with radius equal to 1; $\exp(i\alpha_c)$ is a tangent vector in z_0 along the traversing path. The next term in Eq. (23), namely

$$J_{2K} \equiv \int_Q p(\tau) dk_2(\tau, t), \tag{A4}$$

is transformed to a hypersingular integral. If Q is a straight element then

$$J_{2K} = \exp(2i\alpha_c)(t' - \bar{t}') I_p(\bar{t}'), \tag{A5}$$

with

$$I_p(\bar{t}') = \int_{-1}^1 \frac{p(\tau') d\tau'}{(\tau' - t')^2},$$

is a hypersingular integral defined in Ref. [1,2]. If Q is a circular element then

$$J_{2K} = \frac{\exp(2i\alpha_c)}{\bar{t}'} \left[\int_b^b p(\tau') d\tau' + \frac{1}{\bar{t}'} \left(t' - \frac{1}{\bar{t}'} \right) I_p(1/\bar{t}') \right], \tag{A6}$$

with $b = \exp(i\theta_0)$. The last term for integration of the potential p in Eq. (23) is as follows

$$J_{3K} \equiv \int_Q \frac{p(\tau)}{\tau - \bar{t}} d\tau = \exp(2i\alpha_c) S_p(\bar{t}'), \tag{A7}$$

for a straight element, and

$$J_{3K} = \frac{\exp(2i\alpha_c)}{\bar{r}} \left[\int_b^b p(\tau') d\tau' + \frac{1}{\bar{r}} S_p(1/\bar{r}') \right], \quad (A8)$$

for a circular element.

The integrals of the normal derivative of potential $q = \partial p / \partial n$ have their kernels defined by Eq. (24). The second of them may be transformed to the basic integrals like above

$$J_{2L} \equiv \int_Q q(\tau) k_2(\tau, t) ds. \quad (A9)$$

If Q is a straight element then $ds = l d\tau'$. The kernel k_2 defined by Eq. (12) may be transformed to the local coordinates yielding the following formulae for this integral

$$J_{2L} = l \exp(2i\alpha_c) \left[\int_{-1}^1 q(\tau') d\tau' + (\bar{r}' - t') S_q(1/\bar{r}') \right]. \quad (A10)$$

In the case of a circular element $ds = R d\theta = -iR d\tau'/t'$ (we take into account that $\tau' = \exp(i\theta)$). Then, after algebraic transformation of the kernel, Eq. (A10) becomes

$$J_{2L} = iR \frac{\exp(2i\alpha_c)}{\bar{r}} \left[- \int_b^b q(\tau') d\tau' + \left(t' - \frac{1}{\bar{r}'} \right) S_q(1/\bar{r}') \right]. \quad (A11)$$

The case of the integral with logarithmic kernel is not so simple. For this case, the advantages mentioned above of the CV methods are absent. In the case of a straight element, an analytical formula is available when the density q is a power function of the local coordinate τ' : $q = \tau'^k$ with $k \geq 0$. But, for a circular element one has to present the density as a truncated series of powers with positive and negative k that leads to the numerical calculation of a polylogarithm function.

Starting now with the case of a straight element: $ds = l d\tau'$ and $r^2 = l^2(\tau' - t')(\bar{\tau}' - \bar{t}')$. Then

$$J_{1L} \equiv \int_Q q(s) \ln r^2 ds = l \left[2 \ln l \int_{-1}^1 q(\tau') d\tau' + \int_{-1}^1 q(\tau') \ln(x^2 + a^2) d\tau' \right], \quad (A12)$$

where $x = \tau' - r$; $r = \text{Re } t'$; $a = \text{Im } t'$. Supposing that the density q is presented locally by the truncated Taylor's series, the standard integral that is to be performed is as follows

$$\int_{-1-r}^{1-r} (x+r)^k \ln(x^2+a^2) dx = \sum_{l=0}^k C_k^l r^l \int_{-1-r}^{1-r} x^{k-l} \ln(x^2+a^2) dx. \quad (A13)$$

So, for any $k \geq 0$ and any $l \leq k$ we have a standard integral from a mathematical handbook.

As mentioned above, in the case of a circular element the density approximation includes both positive and negative exponents. Of course, there are some useful

recurrent formulae for reducing integrals with high powers to those of lower exponents. However, the integral of type $\int_{-1-r}^{1-r} x^{-1} \ln(x^2 + a^2) dx$ should be calculated numerically. This consideration leads to conventional numerical schemes if the point t does not belong to the element over which the integration is performed. When the point does fall on the element, we have to separate the element into three parts. Two of them are on the peripheral regions and the third including the t -point is the central one (Fig. A1). The kernel for the third one is expanded using Taylor's series. It is important that r^2 is a small number here. Also, the density can be presented as a truncated series of trigonometric functions because of the following entity

$$c_{-k} \tau'^{-k} + c_k \tau'^k = c_{-k} \exp(-ik\theta) + c_k \exp(ik\theta) = (c_{-k} + c_k) \cos k\theta + (c_k - c_{-k}) \sin k\theta. \quad (A14)$$

Also, $r^2 = R^2(\tau' - t')(\bar{\tau}' - \bar{t}') = R^2[1 - 2d \cos(\theta - \varphi) + d^2]$, where $d = |t'|$, $\varphi = \arg(t')$.

Then, a truncated series of terms is to be integrated. A typical one is as follows

$$\int_{-\theta_0}^{\theta_0} \ln r^2 \cos k\theta d\theta = \ln R^2 \int_{-\theta_0}^{\theta_0} \cos k\theta d\theta + \int_{-\theta_0}^{\theta_0} \ln(1 - 2d \cos \omega + d^2) \cos k\theta d\theta = J_1 + J_2, \quad (A5)$$

with $\omega = \theta - \varphi$. The first integral is an elementary one. The second integral after decomposition of the segment $\varphi \in (-\theta_0, \theta_0)$ yields

$$J_2 = \int_{-\theta_0}^{\varphi-\varepsilon} + \int_{\varphi-\varepsilon}^{\varphi+\varepsilon} + \int_{\varphi+\varepsilon}^{\theta_0} = J_2^1 + J_2^2 + J_2^3, \quad (A16)$$

where ε is a small angle defining the interval of singularity. The first and third integrals are calculated using Gauss quadratures. Then, for $t' = \exp(i\varphi)$, $d = 1$, $\varphi \in (-\theta_0, \theta_0)$, and ω being a small angle $\ln r^2 = \ln(2 - 2 \cos \omega) \approx \ln \omega^2 \approx 2[|\omega| - 1 - (|\omega| - 1)^2/2]$. Then

$$J_2^2 = 2 \int_{\varphi-\varepsilon}^{\varphi+\varepsilon} \cos k\theta [|\omega| - 1 - (|\omega| - 1)^2/2] d\theta = 2 \int_{-\varepsilon}^{\varepsilon} \cos k(\varphi + \omega) F(\omega) d\omega, \quad (A17)$$

where

$$F(\omega) = \omega - 1 - \frac{1}{2}(\omega^2 - 2\omega + 1) = -\frac{\omega^2}{2} + 2\omega - \frac{3}{2},$$

if $\omega \geq 0$,

and

$$F(\omega) = -\omega - 1 - \frac{1}{2}(\omega^2 + 2\omega + 1) = -\frac{\omega^2}{2} - 2\omega - \frac{3}{2},$$

if $\omega < 0$.

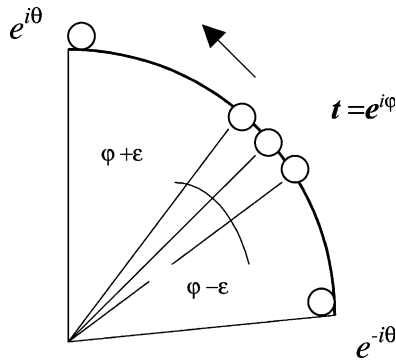


Fig. A1. Decomposition of the integration interval containing the field point.

As a result, we have the truncated series of integrals with exponents multiplied by trigonometric functions; all of which can be found in mathematical handbooks.

The necessity of numerical integration takes away from the usual advantages of CV-BEM techniques. This is because of the special form of the particular solution, Φ in Eq. (7). Another approach suggested by Linkov [13] provides a remedy and avoids numerical integration.

References

- [1] Linkov AM, Mogilevskaya SG. Complex hypersingular BEM in plane elasticity problems. In: Sladek V, Sladek J, editors. *Singular integrals in boundary element methods*. Southampton: Computational Mechanics Publications; 1997. p. 299–364.
- [2] Linkov AM. *Boundary integral equations in elasticity theory*. Dordrecht: Kluwer Academic Publishers; 2002.
- [3] Tanaka M, Sladek V, Sladek J. Regularization techniques applied to boundary element methods. *Appl. Mech. Rev.*, ASME 1994;47(10): 457–99.
- [4] Chen JT, Hong HK. Review of dual boundary element methods with emphasis on hypersingular integrals and divergent series. *Appl. Mech. Rev.*, ASME 1999;52(1):17–33.
- [5] Nowacki W. *Thermoelasticity*. Oxford: Pergamon Press; 1986.
- [6] Hromadka TV, Whitley RJ. *Advances in the complex variable boundary element methods*. New York: Springer; 1997.
- [7] Biot MA. General theory of three-dimensional consolidation. *J. Appl. Phys.* 1941;12:155–64.
- [8] Detournay E, Cheng AH-D. Fundamentals of poroelasticity. In: Fairhurst C, editor. *Comprehensive rock engineering: principles, practice & projects. II. Analysis and design method*. Oxford: Pergamon Press; 1993. p. 113–71. [Chapter 5].
- [9] Banerjee PK. *The boundary element methods in engineering*. London: McGraw-Hill; 1994.
- [10] Rabotnov YuN. *Solids mechanics*. Moscow: Nauka; 1988. (in Russian).
- [11] Erdogan F, Gupta GD, Ratwani M. Interaction between a circular inclusion and an arbitrary oriented crack. *ASME J. Appl. Mech.* 1974; 41:1007–13.
- [12] Helsing J, Jonsson A. On the accuracy of benchmark tables and graphical results in the applied mechanics literature. *ASME J. Appl. Mech.* 2002;69:88–90.
- [13] Linkov AM. The complex variable boundary element method in computational micromechanics. II. *Symposium Mechaniki Zniszczenia Materialow I Konstrukcji*. Augustov, 4–7 czerwca; 2003.